Infrared optical anisotropy of diluted magnetic Ga$_{1-x}$Mn$_x$N/c-sapphire epilayers grown with a GaN buffer layer by metalorganic chemical vapor deposition

Z. G. Hu,[1] A. B. Weerasekara,[1] N. Dietz,[1] A. G. U. Perera,[1,*] M. Strassburg,[1,2] M. H. Kane,[2,3]
A. Asghar,[2] and I. T. Ferguson[2,3]

[1]*Department of Physics and Astronomy, Georgia State University, Atlanta, Georgia 30303, USA*
[2]*School of Electrical and Computer Engineering, Georgia Institute of Technology, Atlanta, Georgia 30332, USA*
[3]*School of Materials Science and Engineering, Georgia Institute of Technology, Atlanta, Georgia 30332, USA*

Optical anisotropy of hexagonal Ga$_{1-x}$Mn$_x$N (x from 0.0% to 1.5%) epitaxial films grown on c-plane sapphire substrates has been investigated using far- and mid-infrared s- and p-polarized reflectance spectra at oblique incidence (at 10°, 22°, and 32°, respectively). The experimental data at room temperature can be well reproduced simultaneously in the measured frequency region of 200–2000 cm^{-1} (5–50 μm), which was based on a four-phase layered system using a 4×4 matrix method [M. Schubert, Phys. Rev. B **53**, 4265 (1996)]. The lattice vibrations perpendicular and parallel to the optic c axis (E_1 and A_1 modes) were expressed by Lorentz oscillator dielectric function model. There was a striking absorption dip at the A_1 phonon frequency in p-polarized reflectance spectra due to the optical anisotropy. These infrared-active phonon parameters were obtained with uniaxial dielectric tensor. It was found that the A_1 longitudinal-optical phonon frequency linearly increases with the Mn composition for the diluted magnetic semiconductor epilayers. The broadening values of the A_1 phonon changed from 3.6 ($\pm$1.3) to 9.0 ($\pm$1.6) cm^{-1}, showing the high film crystal quality. Moreover, the ordinary and extraordinary dielectric functions $\varepsilon_\perp$ and $\varepsilon_\parallel$ of the epilayers were determined. It indicated that $\varepsilon_\parallel$ was larger than $\varepsilon_\perp$ for the Ga$_{1-x}$Mn$_x$N films in the reststrahlen region, which can be ascribed to slight structural degradation of the wurtzite lattice.

I. INTRODUCTION

There has been an increased interest in transition-metal doped wide-band-gap materials, which was amplified by theoretical predictions suggesting that ferromagnetism of diluted magnetic semiconductors (DMSs) with Curie temperatures above room temperature (RT) could be obtained.[1] The DMS materials with a novel interplay in the electronic functionality of semiconductors are of interest due to their unique electrical and magnetic properties.[2–4] Moreover, DMS materials based on III-V group semiconductors have attracted considerable interest as materials that can support the transport and storage of spin and that can be integrated into existing electronic and optoelectronic devices.[5–9] Among these DMS materials, manganese (Mn)-incorporated GaN (Ga$_{1-x}$Mn$_x$N) attracted much attention due to potential for room-temperature ferromagnetism predicted by the Zener model.[4,9–11] It indicates that the strongly localized spins (S =5/2) of the Mn 3d^5 electrons can couple with free carriers, resulting in an effective Mn-Mn ferromagnetic interaction.[4,7] Reports on electronic and magnetic properties of Ga$_{1-x}$Mn$_x$N films have been presented recently.[12,13] A shift in the position of Fermi level with different Mn concentrations was observed together with a ferromagnetic behavior in the Ga$_{1-x}$Mn$_x$N films at RT.[9,13] In those studies, much effort has been focused on analyzing the Mn level transition energies by optical measurements in the ultraviolet-visible region.[9,14,15] However, the analysis of the infrared (IR) optical properties of the Ga$_{1-x}$Mn$_x$N epilayers is still insufficient.

Lattice vibrations and IR dielectric functions of wide-band-gap Ga$_{1-x}$Mn$_x$N films not only provide basic optical properties but will also be critical for developing the novel materials for optoelectronic applications.[16] Phonon and free-carrier properties of the individual layer, such as crystal quality, optical anisotropy, carrier concentration, and mobility, are crucial for GaN-based far-IR (terahertz) detectors with multiple layer structure.[17,18] Moreover, the ferromagnetism of these DMS materials is widely considered to be carrier mediated.[5] Thus, free-carrier characteristics play an important role in optical and electronic behavior of Ga$_{1-x}$Mn$_x$N materials. A prerequisite for the determination of free-carrier concentrations is the accurate knowledge of the phonon modes and dielectric constants of undoped hexagonal Ga$_{1-x}$Mn$_x$N materials.[17] It is known that both E_1 and A_1 phonon modes (perpendicular and parallel to optic c axis, respectively) at the Brillouin-zone center are IR active in wurtzite GaN-based semiconductor films with the space group C_{6v}^4.[19,20] Optical behavior of these polar modes is particularly interesting because of important effects from Mn incorporation with the GaN host lattice. Recently, we reported the effects of Mn composition on the E_1 phonon of undoped Ga$_{1-x}$Mn$_x$N films.[21] However, the A_1 mode and optical anisotropy could not be resolved due to the application of s-polarized incident light. This is according to the fact that A_1 phonon, which is parallel to the optic c axis, cannot be excited by the incident light perpendicular to the plane of incidence.[22–24] Note that there are some deviations from the c axis for p-polarized light at larger angles of incidence. In this case, optical anisotropy of hexagonal materials can be obtained theoretically due to nonzero component from the light parallel to the plane of incidence, which essentially requires two dielectric functions (i.e., ordinary and extraordinary parts) for uniaxial films.[25]

For films with thickness significantly less than incident IR wavelength, the longitudinal-optical (LO) phonon shows a

minimum dip in reflectance and/or transmittance spectra, which is known as Berreman's effect.[26,27] Wetzel *et al.* observed the A_1(LO) phonon mode of Al$_x$Ga$_{1-x}$N films on *c*-sapphire; Berreman's effect was taken into account to interpret the phenomena although detailed calculations were not given in the above work.[24] According to the previous investigations on GaN films, the frequencies of the E_1(LO) and A_1(LO) phonons are located in energy regions of 738–746 and 730–744 cm^{-1}, respectively.[19,22,24,28–30] Distinguishing the two effects is difficult due to different film thicknesses and the experimental configurations. Therefore, it is necessary to further clarify them for hexagonal Ga$_{1-x}$Mn$_x$N expilayers from Mn influences. It is worthwhile to note that Berreman's effect and optical anisotropy are very sensitive to the angle of incidence. Although Kasic *et al.* investigated the anisotropic behavior of doped GaN films by IR ellipsometry,[19] no studies are reported on IR optical anisotropy of diluted magnetic Ga$_{1-x}$Mn$_x$N epilayers.

In this paper, IR optical anisotropic properties of the Ga$_{1-x}$Mn$_x$N films are investigated using *s*- and *p*-polarized reflectance spectra at oblique angles of incidence. Based on a detailed theoretical analysis and fitting calculation, the influences of Mn incorporation on the E_1 and A_1 phonon modes and on the anisotropic dielectric functions are discussed.

II. EXPERIMENTAL DETAILS

A. Growth of Ga$_{1-x}$Mn$_x$N films

Hexagonal Ga$_{1-x}$Mn$_x$N epilayers with the composition ranging from $x=0.3\%$ to 1.5% were deposited near standard GaN growth temperatures on *c*-sapphire substrates with a GaN buffer layer by metal organic chemical vapor deposition (MOCVD). The growth of high quality Ga$_{1-x}$Mn$_x$N on sapphire without a GaN seed/nucleation layer (GaN buffer layer) not only is very difficult but also will introduce additional modification in the optical properties which are related to Ga$_{1-x}$Mn$_x$N/sapphire interface. The crystalline quality of the expitaxial films was studied[8] by high-resolution x-ray diffraction (HRXRD). The full width at half maximum of the (0002) peak for samples incorporated at a Mn composition of about 1% is 150 arc sec, which is slightly below the value of 179 arc sec recorded for the GaN film, confirming the high

crystalline quality. Details of the growth process and the structural characterizations are given in Refs. 8 and 13.

B. Polarized infrared spectral measurements

Far-IR (FIR) and mid-IR (MIR) reflectance spectra at oblique incidence were measured with *s*- and *p*-polarized light over the frequency range of 200–2000 cm^{-1} (5–50 μm) using a nitrogen purged Perkin-Elmer system 2000 Fourier transform infrared spectrometer.[16] For the MIR region of 450–2000 cm^{-1}, a liquid-nitrogen-cooled mercury cadmium telluride detector and optimized KBr beam splitter were used with a spectral resolution of 4 cm^{-1}. A TGS/POLY detector and 6-μm-thick Mylar beam splitter were employed for the measurements in the FIR region of 200–700 cm^{-1} with the same resolution. Reflectance spectra were recorded using spectral reflectance accessory (Graseby Specac Ltd.). Three incident angles (10°, 22°, and 32°) with respect to the plane of incidence were selected to improve the fitting reliability and quality. A wire grid KRS-5 polarizer and polyethylen polarizer were used to obtain the polarized light in the MIR and FIR ranges, respectively. Gold (Au) and aluminum (Al) mirrors, whose absolute reflectances were directly measured, were taken as references for the spectra in the MIR and FIR regions, respectively. The samples were kept at RT for all measurements and no mathematical smoothing has been performed for the experimental reflectance data.

III. RESULTS AND DISCUSSION

A. Theoretical considerations

A matrix method, where optical component of each layer is expressed by a 4×4 matrix, is proved to be sufficient in order to calculate optical response of anisotropic media.[25] Suppose the dielectric function of anisotropic film in the *x*-*y* plane (perpendicular to the *c* axis, $\varepsilon_x = \varepsilon_y$) is $\varepsilon_\perp$, the dielectric function in the *z* plane (parallel to the *c* axis) $\varepsilon_\parallel$, unity for vacuum, and substrate ε_s, respectively. In the present work, the anisotropy of the sapphire substrate is neglected to simplify the simulation, which has no effect on the determination of the E_1 and A_1 phonon modes.[16] The resultant matrix M_r is described by the following product: $M_r = M_{in}M_1M_2M_{ex}$.[25] Here, M_{in} and M_{ex} are the incident and exit matrices, respectively. It is easy to calculate them by taking optical isotropy of vacuum and substrate into account. M_1 and M_2 are the propagation matrix $T(d)^{-1}$ expressing optical properties of the Ga$_{1-x}$Mn$_x$N layer and GaN template underlying, which has a general form[25]

$$T = \begin{bmatrix} \cos(2\pi d\tilde{N}_{xz}/\lambda) & 0 & 0 & i(\tilde{N}_{xz}/\varepsilon_x)\sin(2\pi d\tilde{N}_{xz}/\lambda) \\ 0 & \cos(2\pi d\tilde{N}_{yy}/\lambda) & -i(1/\tilde{N}_{yy})\sin(2\pi d\tilde{N}_{yy}/\lambda) & 0 \\ 0 & -i\tilde{N}_{yy}\sin(2\pi d\tilde{N}_{yy}/\lambda) & \cos(2\pi d\tilde{N}_{yy}/\lambda) & 0 \\ i(\varepsilon_x/\tilde{N}_{xz})\sin(2\pi d\tilde{N}_{xz}/\lambda) & 0 & 0 & \cos(2\pi d\tilde{N}_{xz}/\lambda) \end{bmatrix}, \quad (1)$$

where d is the film thickness, λ is the incident wavelength, and $\widetilde{N}_{xz}$ and $\widetilde{N}_{yy}$ can be calculated using Snell's law with the incident angle φ,

$$\widetilde{N}_{xz} = \sqrt{\varepsilon_x}\sqrt{1 - [(1/\sqrt{\varepsilon_z})\sin\varphi]^2},$$

$$\widetilde{N}_{yy} = \sqrt{\varepsilon_y}\sqrt{1 - [(1/\sqrt{\varepsilon_y})\sin\varphi]^2}. \qquad (2)$$

The s and p-polarized reflectance can be readily obtained,

$$R_s = \left| \frac{M_{r10}M_{r22} - M_{r12}M_{r20}}{M_{r00}M_{r22} - M_{r02}M_{r20}} \right|^2,$$

$$R_p = \left| \frac{M_{r30}M_{r02} - M_{r32}M_{r00}}{M_{r20}M_{r02} - M_{r22}M_{r00}} \right|^2. \qquad (3)$$

It should be emphasized that s-polarized spectrum R_s, which has the information only about the ordinary dielectric function, shows similar spectral shape under different angles of incidence except for the reflectance intensity. However, the p-polarized spectrum R_p, which is more sensitive to the parallel dielectric response even at small incident angles, is required to obtain the optical anisotropy.

In the simulation, a three-phase layered model (air/GaN/sapphire) was used for the GaN buffer layer. The obtained fitting parameters were fixed in all subsequent four-phase model calculations for the $Ga_{1-x}Mn_xN$ epilayers (air/$Ga_{1-x}Mn_xN$/GaN/sapphire).[21] Compared with isotropic structure, the dielectric tensor ε is necessary to completely describe the optical response of uniaxial media,[20,27]

$$\varepsilon = \begin{bmatrix} \varepsilon_x & & \\ & \varepsilon_y & \\ & & \varepsilon_z \end{bmatrix} = \begin{bmatrix} \varepsilon_\perp & & \\ & \varepsilon_\perp & \\ & & \varepsilon_\parallel \end{bmatrix}. \qquad (4)$$

For polar semiconductor materials, IR dielectric response can be expressed by the harmonic Lorentz oscillator model, in which the dielectric function is defined as a response function having many pairs of simple poles,[16,20–22]

$$\varepsilon(\omega)_{\perp,\parallel} = \varepsilon_{\infty\perp,\parallel} + \frac{\varepsilon_{\infty\perp,\parallel}(\omega_{LO\perp,\parallel}^2 - \omega_{TO\perp,\parallel}^2)}{\omega_{TO\perp,\parallel}^2 - \omega^2 - i\omega\Gamma_{TO\perp,\parallel}}. \qquad (5)$$

Here, ε_∞, ω_{LO}, ω_{TO}, Γ_{TO}, and ω represent, in order, high-frequency dielectric constant, LO phonon frequency, transverse-optical (TO) phonon frequency, broadening values of TO phonons, and incident light frequency. The subscripts "$\perp$" and "$\parallel$" represent the dielectric functions perpendicular ($\varepsilon_\perp$) and parallel ($\varepsilon_\parallel$) to the optic c axis, respectively. It is a challenge to simulate IR reflectance spectra of anisotropic multilayer system with similar optical properties, e.g., GaN and $Ga_{1-x}Mn_xN$ with low Mn compositions, under multiple angles of incidence because there is a stronger parameter correlation due to closer phonon frequencies. Therefore, Lorentz oscillator model containing less fitting parameters could be desirable in the simulations, as compared with IR ellipsomtry.[19] Free-carrier effects are neglected since the $Ga_{1-x}Mn_xN$ epilayers are nominally undoped, which are confirmed by Raman scattering (an upper limit of 10^{16} cm^{-3}).[9,13] The best-fit parameter values in Eq. (5) can be found using a
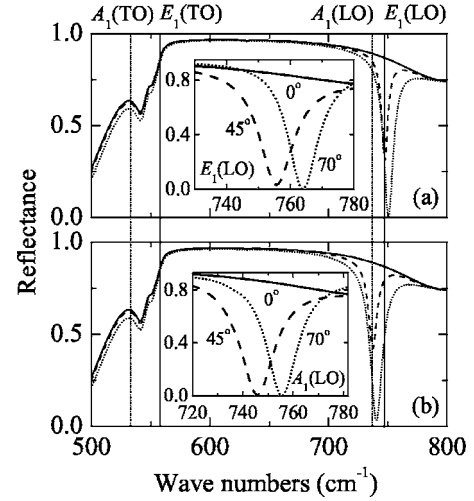

FIG. 1. Calculated p-polarized infrared spectra R_p corresponding to (a) Berreman effect and (b) optical anisotropy of the GaN film on sapphire at different angles of incidence. The solid, dashed, and dotted lines represent the data at the incident angles of 0°, 15°, and 30°, respectively. The insets show the R_p reflectance at larger angles of incidence in the E_1(LO) and A_1(LO) phonon frequency regions, respectively.

Levenberg-Marquardt algorithm, which is an efficient non-linear calculation method for many parameter fitting.[16]

B. Berreman effect and optical anisotropy

A comprehensive approach to analyze the anisotropy of hexagonal GaN is complicated because of p- and s-light coupling at medium interface.[25] However, an assumption that the c axis is perpendicular to the sample surface can greatly simplify the calculation due to no cross conversion between p- and s-polarized light [see Eq. (1)].[27] Figure 1 shows the calculated spectra R_p of the GaN film on sapphire at different angles of incidence (from 0° to 70°). The film thickness (2.1 μm) and dielectric function parameters are taken from the simulation procedure (Sec. III C). For the present GaN epilayer, the E_1(LO) and E_1(TO) phonons are located at 746.4 and 558.4 cm^{-1}, respectively. From Fig. 1(a), there are no obvious differences among the reflectance spectra corresponding to different incident angles varying from 0° to 30° except for the E_1(LO) position, where a minimum dip increases with the angle. This can be ascribed to the known Berreman's effect due to some practically parallel components from electrical field, which excites the LO mode at nonzero angle of incidence.[26] Note that the dip is sensitive to the incident angle. As Tiwald *et al.* stated, the behavior from thick epilayers is similar to that of bulk crystal because phonon damping limits the penetration depth of the IR light.[27] However, the E_1(LO) position will shift to the high-energy side if the thickness decreases and/or the angle of incidence increases, as shown in the inset of Fig. 1. It is found that the variation can approach about 15 cm^{-1} with the applied angles, which indicates that the E_1(LO) phonon can be directly detected based on Berreman's effect.

The optical response becomes complex for anisotropic materials. The parallel dielectric function mainly contributes
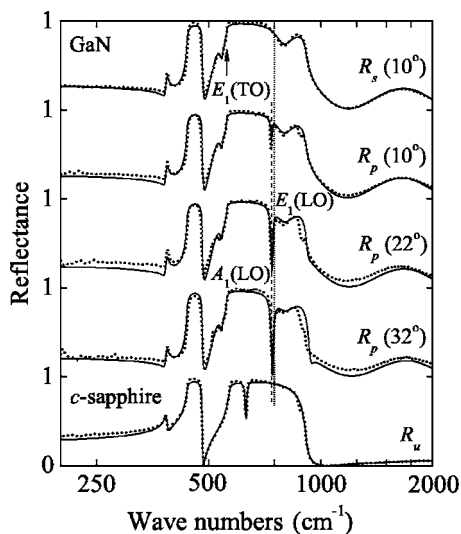
FIG. 2. Experimental infrared reflectance spectra (dotted lines) of the GaN film and sapphire, and their best-fit results (solid lines) at oblique incidence. Note that *s*-polarized spectra R_s and *p*-polarized spectra R_p are used for the GaN sample, whereas unpolarized spectra R_u at near-normal incidence are used for the sapphire substrate. The straight dotted and dashed lines indicate the $E_1(LO)$ and $A_1(LO)$ phonon frequencies, respectively. The horizontal coordinate is the logarithmic unit to enlarge the reststrahlen region.

to the reflectance spectra when the $A_1(LO)$ phonon frequency is close to the $E_1(LO)$ phonon frequency. From Fig. 1(b), the $E_1(LO)$ phonon feature disappears and the $A_1(LO)$ phonon can be observed at the corresponding position. This agrees with the results of doped GaN films grown on sapphire substrate by IR ellipsometry and polarized reflectance spectra.[19,29] Similarly, the $A_1(LO)$ phonon mode (737.0 cm^{-1}) shows a minimum dip, which is sensitive to the angle of incidence. Obviously, the dip in the reflectance spectra is not from the $E_1(LO)$ phonon for hexagonal GaN. Nevertheless, the spectra cannot give any information on the $A_1(TO)$ phonon mode owing to polarized light and angles of incidence.[19,29] From the theoretical calculations, the reststrahlen band (nearly total reflection) of the GaN epilayer always starts from the $E_1(TO)$ mode independent of angles of incidence, which results in an undistinguished feature for the $A_1(TO)$ mode (see the straight dotted line in Fig. 1). The values of spectra R_s are larger than those of R_p at the corresponding angle and increase with the angle of incidence in the reststrahlen region (not shown here). It should be noted that *s*-polarized spectra R_s are not sensitive to Berreman's effect and optical anisotropy, regardless of angles of incidence.

As an experimental verification, the measured reflectance spectra of the GaN buffer layer using *s*- and *p*-polarized incident light together with their fit have been presented in Fig. 2. The unpolarized spectrum R_u at near-normal incidence of *c*-sapphire substrate has also been plotted for comparison, which can be satisfactorily reproduced with an isotropic model.[16] Compared with the spectrum R_s, there is a striking dip at about an energy of 736 cm^{-1} (high-energy shift under a larger angle of incidence) in the spectra R_p of
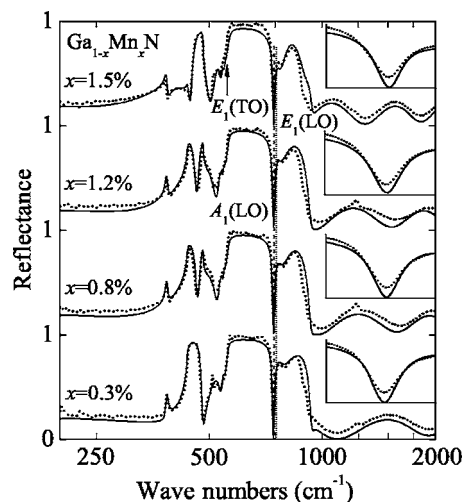
the GaN layer. A fitting calculation was initially performed for the spectrum R_s; the $E_1(LO)$ phonon frequency is found to be 746.4 cm^{-1}, which agrees with the previous values.[22,28,30] Therefore, it can be concluded unambiguously that the above absorption dip is due to the optical anisotropy, i.e., the $A_1(LO)$ phonon other than the $E_1(LO)$ mode. An isotropic treatment is no longer valid and an optical anisotropic description has to be taken into account in order to extract the sharp feature.

C. Reflectance spectra at oblique incidence

Before carrying out fitting on IR reflectance spectra of $Ga_{1-x}Mn_xN/GaN/sapphire$ systems, simulations on IR data of GaN/sapphire were performed and relevant parameters for the GaN epilayer were obtained first. Thereafter, calculations were followed on the reflectance spectra of $Ga_{1-x}Mn_xN/GaN/sapphire$ epilayers by fixing parameters obtained for the GaN buffer layer. Having a well defined, stable GaN surface, the effect of Mn incorporation in the upper $Ga_{1-x}Mn_xN$ layers can be analyzed using the differential approach. The experimental and fitting of *p*-polarized reflectance spectra at an incident angle of 32° for the $Ga_{1-x}Mn_xN$ epilayers with the composition *x* from 0.3% to 1.5% are shown in Fig. 3 by dotted and solid lines. The reflectance spectra R_p for other two angles are not shown due to the fact that they do not carry any extra information. For all epilayers, the sharp dip induced by the $A_1(LO)$ phonon can be observed at a wavenumber value of about 736 cm^{-1}. As previously stated, the characteristics are due to the optical anisotropy in the $Ga_{1-x}Mn_xN$ films and GaN template underlying. This is ascribed to *p*-polarized light of nonperpendicular incidence in the hexagonal epilayers, which can be interacted with the A_1 phonon mode and make it IR active. The results were confirmed by complementary techniques such as Raman scattering.[13]

The simulation procedure can be carried out by the following steps: (1) the E_1 phonon modes of the epilayers were

FIG. 3. Experimental infrared reflectance spectra R_p (dotted lines) of the $Ga_{1-x}Mn_xN$ films on the GaN/sapphire and their best-fit results (solid lines) at an incident angle of 32°. The insets show an enlarged fitting region of the $A_1(LO)$ phonon mode.

TABLE I. The parameter values of the Lorentz oscillator model for the E_1 and A_1 phonon modes of the $Ga_{1-x}Mn_xN$ films as determined from the fitting of polarized infrared reflectance spectra in Figs. 2 and 3. The 90% reliability of the fitting parameters is given in parentheses. Note that $\varepsilon_{\infty\parallel}$ is equal to $\varepsilon_{\infty\perp}$. The ω_{TO} of the A_1 phonon remains at 533 cm^{-1} from Raman scattering. The parameters ε_∞ and ε_0 are dimensionless and all other parameters are in cm^{-1}.

Samples	x (%)	E_1 phonon					A_1 phonon		
		$\varepsilon_{\infty\perp,\parallel}$	$\varepsilon_{0\perp}$	ω_{LO}	ω_{TO}	Γ_{TO}	$\varepsilon_{0\parallel}$	ω_{LO}	Γ_{TO}
1317u	0.0	5.08	9.08	746.4	558.4	5.0	9.70	736.2	7.2
		(0.03)	(0.11)	(1.7)	(0.6)	(0.2)	(0.06)	(0.2)	(0.5)
1128m	0.3	5.18	9.22	747.2	560.0	7.0	9.88	736.1	3.6
		(0.06)	(0.21)	(3.4)	(0.6)	(0.6)	(0.14)	(0.6)	(1.3)
1131m	0.8	5.16	9.10	746.4	562.2	6.9	9.85	736.5	5.9
		(0.04)	(0.14)	(1.8)	(0.8)	(0.3)	(0.08)	(0.4)	(1.1)
1133m	1.2	5.25	9.11	740.8	562.5	7.0	10.05	737.3	9.0
		(0.05)	(0.16)	(2.2)	(0.9)	(0.4)	(0.11)	(0.6)	(1.6)
1215m	1.5	5.22	9.12	745.0	563.7	9.6	9.98	736.8	5.2
		(0.04)	(0.13)	(1.3)	(0.8)	(0.3)	(0.08)	(0.3)	(0.8)

determined by fitting the spectra R_s at near-normal incidence, that cannot interact with the LO modes and have better signal output compared with those at larger angles of incidence; (2) with the three-phase layered model, the $A_1(LO)$ phonon parameter values of the GaN buffer layer were derived by fitting the R_p data recorded at the incident angles of 10°, 22°, and 32°; (3) the $A_1(LO)$ phonon frequency and broadening value of the $Ga_{1-x}Mn_xN$ epilayers can be obtained by fitting the R_p data under three incident angles simultaneously with the known parameters of the GaN epilayer and the E_1 phonons. It should be emphasized that the phonon frequency variations of the $Ga_{1-x}Mn_xN$ films are reasonably from Mn contributions because the GaN buffer layer is the same and the information from it was kept unchanged in the simulations. Note that the parallel high-frequency dielectric constant $\varepsilon_{\infty\parallel}$ is considered as the same value as $\varepsilon_{\infty\perp}$ (i.e., isotropic treatment).[20,22] In all calculations, the $A_1(TO)$ phonon frequency is assumed to be 533 cm^{-1} and does not shift from Raman scattering.[13]

The calculated results based on the optical anisotropic model are in good agreement with the measured spectra R_p, as shown by solid lines in Figs. 2 and 3, even in the $A_1(LO)$ phonon frequency region (see the insets of Fig. 3). It should be stated that the R_p data from the $Ga_{1-x}Mn_xN$ epilayers at the incident angles of 10° and 22° are not displayed due to the similar behavior. The fitting standard deviations of the epilayers[16] are less than 1.5×10^{-3} for all three angles. It indicates that the present model calculations have a good convergence and fitting quality within the experimental errors. The fitted parameters with the Lorentz oscillator model for the E_1 and A_1 phonons are summarized in Table I. The thickness of the $Ga_{1-x}Mn_xN$ epilayers varies from 0.34 to 1.7 μm, which can be compared with the nominal growth values.[9,13] For the two samples with Mn compositions of 0.3% and 0.8%, the thickness obtained by the spectra R_s is slightly different from that by the spectra R_p. The deviation values are 8%, and 16%, respectively. This is owing to thickness nonuniformity of the films, which are deposited

on the sapphire wafer with a diameter size of 2.0 in. and different incident light spot positions.

As shown in Fig. 4(a), the parameter $\varepsilon_{\infty\perp}$ ($=\varepsilon_{\infty\parallel}$) values of the $Ga_{1-x}Mn_xN$ films are larger than that of the GaN layer, indicating that Mn introduction may have affected the high-energy electronic transitions. A weak improvement in the conductivity by Mn acceptor could increase the contributions from the high-energy side, which results in an enhancement of $\varepsilon_{\infty\perp}$ and $\varepsilon_{\infty\parallel}$. It is well known that the static dielectric constants ε_0 are related to the high-frequency dielectric constants by the Lyddane-Sachs-Teller relation: $\varepsilon_{0\perp,\parallel} = \varepsilon_{\infty\perp,\parallel}(\omega_{LO\perp,\parallel}/\omega_{TO\perp,\parallel})^2$.[17,31] The calculated perpendicular and parallel static dielectric constants $\varepsilon_{0\perp}$ and $\varepsilon_{0\parallel}$ are presented in Fig. 4(b). The parallel static dielectric constants are larger than the corresponding perpendicular ones. The pa-
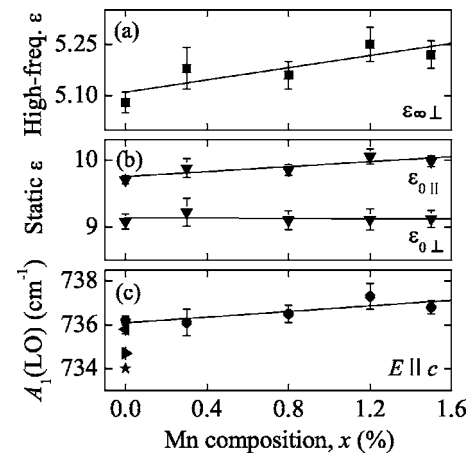

FIG. 4. (a) High-frequency ε_∞, (b) static dielectric constants ε_0, and (c) the $A_1(LO)$ phonon frequencies of the $Ga_{1-x}Mn_xN$ films derived from the Lorentz oscillator model. The solid lines are the linear fitting results to guide the eyes. The symbols "$\perp$" and "$\parallel$" represent the perpendicular (E_1) and parallel (A_1) to the optic c axis, respectively. For comparison, the values "$\blacktriangleleft$," "$\blacktriangleright$," and "$\bigstar$" for GaN in (c) are taken from Refs. 28–30, respectively.

rameters $\varepsilon_{0\perp}$ and $\varepsilon_{0\parallel}$ vary from 9.08 to 9.22 and from 9.7 to 10.05, respectively. The $\varepsilon_{0\perp}$ is less than 9.5; however, the $\varepsilon_{0\parallel}$ is close to 10.4 reported for the GaN film.[22] Moreover, the parallel static dielectric constant $\varepsilon_{0\parallel}$ shows a linear increasing trend with the Mn composition, indicating the electronic influences (e.g., the exciton binding energy) distinctly from Mn incorporation on the GaN host matrix. This is similar to hexagonal $Mg_xZn_{1-x}O$ semiconductor epilayers recently studied by IR ellipsometry.[17]

D. Parallel phonon mode

The effects from small Mn concentrations (Mn^{+2} as a dopant) on basic physical properties, such as Curie temperatures, magnetic properties, free-carrier transports, optical-phonon modes, and band gaps are significant for spin-electronics applications. In order to gain a better insight into the phonon-assisted optical transitions (i.e., indirect-band-gap transitions), zero-center phonon replica, and so-called band-gap engineering for the $Ga_{1-x}Mn_xN$ DMS, magnetic composition dependency of the crystalline lattice dynamics has to be thoroughly investigated. When IR reflectance band is relatively wide, both LO and TO phonon modes may have different phonon decays.[32] This discrepancy can be due to the electric field and displacement on the lattice, which induces phonon mode splitting and damping.[26] From Table I, the $E_1(TO)$ phonon frequency increases linearly with Mn composition. However, the $E_1(LO)$ phonon mode shows a weak composition dependency. The detailed discussions of the E_1 mode can be found in Ref. 21. The $A_1(LO)$ phonon frequencies together with the reported values of the GaN buffer layer are shown in Fig. 4(c). The $A_1(LO)$ phonon frequency is higher than that (734 cm^{-1}) of $Ga_{1-x}Mn_xN$ bulk crystals from Raman scattering.[33]

The $A_1(LO)$ mode frequency increases linearly with the Mn composition in the experimental errors. It was reported that the replacement of Ga atoms by Mn atoms is not expected to lead to a substantial lattice relaxation.[34] As shown, the phonon frequencies do not show a striking variation with the Mn composition. It indicates that there is a relatively small effect on interactions of the lattice vibration with the electric vector parallel to the plane of incidence. Note that the $A_1(LO)$ position is sensitive to the carriers plasma frequency, which is a function of free-carrier concentrations. However, a small increment of the $A_1(LO)$ phonon frequency is intrinsic in the $Ga_{1-x}Mn_xN$ materials because the interactions between the free carriers and LO phonon, which normally result in an additional high-frequency shift, are weak and excluded by Raman scattering as previously stated.[16] Mn nanoscale clusters and/or Ga-site replacements can induce the crystal distortion of the GaN matrix and slight degradation in the $Ga_{1-x}Mn_xN$ structural quality.[13,34] These weak dependencies can be related to low Mn doping levels, which can be further confirmed by the HRXRD results. This fact suggests that the Mn introduction affects the Ga-N atomic displacements parallel to the optic c axis. The Mn-N interactions could be weaker than the Ga-N host lattice vibrations due to different atomic weights and electronic polarizations from Ga and Mn elements. It indicates that there is a slight
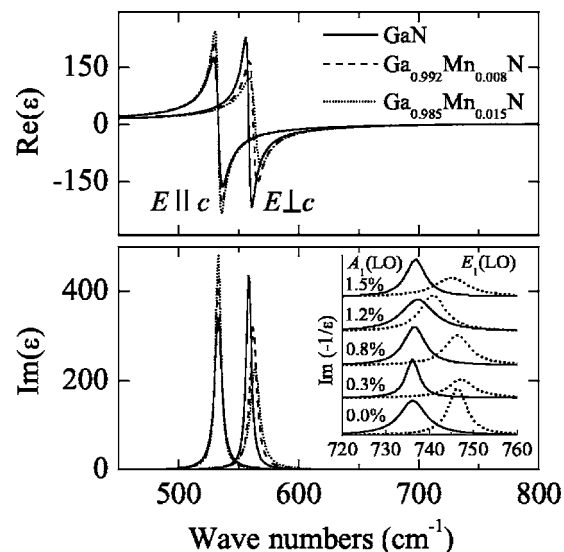

FIG. 5. The infrared anisotropic dielectric functions of the $Ga_{1-x}Mn_xN$ epilayers. For clarity, the evolution of $\varepsilon_{\perp,\parallel}$ with the Mn composition $x=0.0$, 0.8%, and 1.5% are plotted. The inset is an enlargement of the E_1 (dotted lines) and A_1 (solid lines) phonon frequency regions for the energy loss functions $Im(-1/\varepsilon_{\perp})$ and $Im(-1/\varepsilon_{\parallel})$, respectively.

discrepancy between the atomic displacements in the sublattice, which is comprised of Ga-N and/or Mn-N components. Klochikhin *et al.* stated that the Ga-site fluctuations provide a phonon-scattering cross section, which is proportional to the product of the Ga and another element compositions in ternary GaN-based semiconductors.[35] For the $Ga_{1-x}Mn_xN$ epilayers, the $A_1(LO)$ phonon variation theoretically depends on the small value of $x(1-x)$, which contributes to the weak composition dependence observed experimentally. Nevertheless, it could be reasonable that the second term (x^2) can be neglected due to diluted Mn-incorporation (a limit to 1.5%) in the present work. Based on the above analysis, the Mn clustering effect has not been observed with polarized IR reflectance spectra at RT.

E. Dependence of anisotropic dielectric function on Mn composition

The IR dielectric functions are the basic parameters for semiconductor optoelectronic device designs, e.g., spectral responsivity, spectral bandwidth, and threshold frequency of detectors.[36] It can provide an insight on the electronic structure and optical dispersion behavior of semiconductors. Unlike GaAs-based devices, the optical anisotropy plays an important role in designs and achievements for GaN-based IR detectors due to growth directions and substrate orientations.[18,36] Based on the fitted parameter values in Table I, Fig. 5 shows IR anisotropic dielectric functions resulting from the E_1 and A_1 phonon modes for the GaN, $Ga_{0.992}Mn_{0.008}N$, and $Ga_{0.985}Mn_{0.015}N$ epitaxial films in the frequency region of 450–800 cm^{-1}. The perpendicular dielectric function $\varepsilon_{\perp}$ (E_1) is less than the parallel one $\varepsilon_{\parallel}$ (A_1) for the $Ga_{1-x}Mn_xN$ epilayers in the reststrahlen region and

the case is opposite to the behavior of the GaN layer. It indicates that the $Ga_{1-x}Mn_xN$ is uniaxial positive, i.e., $\sqrt{|\varepsilon_\perp|} < \sqrt{|\varepsilon_\parallel|}$, in the reststrahlen region.[37] This may be ascribed to some perturbations of the electronic structures from the Mn introduction, which results in the weak deterioration of crystal anisotropy.

In the transparent region, the $\varepsilon_\perp$ is slightly higher than the $\varepsilon_\parallel$ for the epilayers. At the achieved energy of 2000 cm^{-1} (5 μm), $\varepsilon_\perp$ is 4.86 for the $Ga_{0.985}Mn_{0.015}N$ epilayer, which is larger than values 4.73 from the GaN and 4.82 from the $Ga_{0.992}Mn_{0.008}N$ films. It indicates that the extraordinary refractive indices of these epilayers are about 2.2, which agrees well with the previous reports of the GaN layer. The average difference between ordinary ($E \perp c$) and extraordinary ($E \parallel c$) refractive indices in the transparent range for all epilayers is about 0.4%, which is less than that (3.0%) of the GaN layer in the visible region. The small discrepancy is mainly attributed to the isotropic assumption of the high-frequency dielectric constant ($\varepsilon_{\infty\perp} = \varepsilon_{\infty\parallel}$) in the calculations. It should be stated that fitting $\varepsilon_{\infty\parallel}$ is not successful due to the complicated four-layered system in the present work. More sensitive polarized spectral measurement, such as spectroscopy ellipsometry, can be desirable to determine the anisotropy of ε_∞.[17,19,27]

For the perpendicular dielectric function $\varepsilon_\perp$, the peaks of the real and imaginary parts show a blueshift trend with increasing Mn composition. Moreover, the line shapes of the $Ga_{1-x}Mn_xN$ films are obviously broadened and the intensity becomes weaker, compared with that of a GaN film. As discussed above, the peak value of the GaN film is larger due to a smaller broadening value. However, the behavior is not similar to the parallel dielectric function $\varepsilon_\parallel$, in which only the peak value increases in the reststrahlen region. This could be due to the fixed A_1(TO) phonon mode and the similar broadening parameters. In Eq. (5), the maximum values of the imaginary part of the dielectric function appear at the TO phonon position. However, the function $Im(-1/\varepsilon)$ provides the maximum at the corresponding LO phonon frequency. For the $Ga_{0.985}Mn_{0.015}N$ epilayer, at the TO frequencies the imaginary parts of $\varepsilon_\parallel$ and $\varepsilon_\perp$ are 483 and 228, respectively. Note that the real part of the dielectric function crosses zero at the corresponding TO positions.

The inset of Fig. 5 shows the energy loss functions of $Im(-1/\varepsilon_\perp)$ and $Im(-1/\varepsilon_\parallel)$, which indicate that the peaks are at the E_1(LO) and A_1(LO) phonon frequencies. It was found that the values of the function $Im(-1/\varepsilon_\parallel)$ [A_1(LO)] are larger

than those of the corresponding $Im(-1/\varepsilon_\perp)$ [E_1(LO)] for the $Ga_{1-x}Mn_xN$ epilayers except for the GaN film. The peak of $Im(-1/\varepsilon_\perp)$ from the $Ga_{0.988}Mn_{0.012}N$ film shifts toward the low-energy side and is located at about 740 cm^{-1} (Table I). The sharp A_1(LO) and E_1(LO) features of the $Ga_{0.997}Mn_{0.003}N$ and GaN epilayers are due to the smallest broadening (3.6 and 5.0 cm^{-1}, respectively) and neglected free-carrier effects. It indicates that there is no LO phonon plasmon coupling interaction, which normally separates the LO phonon into two modes with different energies.[16,19] From the present discussions, it can be concluded that Mn incorporation effects are more significant for the properties of the perpendicular dielectric response than the parallel component. Further, detailed polarized spectroscopy is necessary to clarify the optical behavior for the parallel component of the dielectric function.

IV. CONCLUSIONS

The infrared optical properties of $Ga_{1-x}Mn_xN$ ($0.0\% \leq x \leq 1.5\%$) films deposited by MOCVD have been investigated using reflectance spectroscopy at oblique incidence with s- and p-polarized light. Owing to the hexagonal structure, the Berreman effect and the optical anisotropy of the $Ga_{1-x}Mn_xN$ epilayers have been discussed theoretically and analyzed experimentally. An optical anisotropic model was used to obtain the E_1 and A_1 phonon frequencies. The E_1(LO) phonon modes show a weak dependency on the Mn incorporation. However, the A_1(LO) and E_1(TO) phonon frequencies linearly increase with the Mn concentration. The average difference between ordinary and extraordinary refractive indices is found to be about 0.4% in the transparent range. The perpendicular dielectric function is slightly smaller than the parallel one, indicating that the $Ga_{1-x}Mn_xN$ films are uniaxial positive in the reststrahlen region.

*Electronic address: uperera@gsu.edu

[1] T. Dietl, H. Ohno, F. Matsukura, J. Cibert, and D. Ferrand, Science **287**, 1019 (2000).

[2] H. Ohno, Science **281**, 951 (1998).

[3] S. J. Pearton, C. R. Abernathy, M. E. Overberg, G. T. Thaler, D. P. Norton, N. Theodoropoulou, A. F. Hebard, Y. D. Park, F. Ren, J. Kim, and L. A. Boatner, J. Appl. Phys. **93**, 1 (2003).

[4] E. M. Hankiewicz, T. Jungwirth, T. Dietl, C. Timm, and Jairo Sinova, Phys. Rev. B **70**, 245211 (2004).

[5] E. J. Singley, R. Kawakami, D. D. Awschalom, and D. N. Basov, Phys. Rev. Lett. **89**, 097203 (2002).

[6] W. Limmer, M. Glunk, S. Mascheck, A. Koeder, D. Klarer, W. Schoch, K. Thonke, R. Sauer, and A. Waag, Phys. Rev. B **66**, 205209 (2002).

[7] R. Aguado, M. P. López-Sancho, J. Sinova, and L. Brey, Phys. Rev. B **70**, 195201 (2004).

[8] M. H. Kane, A. Asghar, C. R. Vestal, M. Strassburg, J. Senawiratne, Z. J. Zhang, N. Dietz, C. J. Summers, and I. T.

Ferguson, Semicond. Sci. Technol. **20**, L5 (2005).

[9] M. Strassburg, M. H. Kane, A. Asghar, Q. Song, Z. J. Zhang, J. Senawiratne, M. Alevli, N. Dietz, C. J. Summers, and I. T. Ferguson, J. Phys.: Condens. Matter **18**, 2615 (2006).

[10] Z. S. Popovic, S. Satpathy, and W. C. Mitchel, Phys. Rev. B **70**, 161308(R) (2004).

[11] G. Thaler, R. Frazier, B. Gila, J. Stapleton, M. Davidson, C. R. Abernathy, and C. Segre, Appl. Phys. Lett. **84**, 1314 (2004).

[12] M. J. Reed, F. E. Arkun, E. A. Berkman, N. A. Elmasry, J. Zavada, M. O. Luen, M. L. Reed, and S. M. Bedaira, Appl. Phys. Lett. **86**, 102504 (2005).

[13] M. H. Kane, M. Strassburg, A. Asghar, W. E. Fenwick, J. Senawiratne, Q. Song, C. J. Summers, Z. J. Zhang, N. Dietz, and I. T. Ferguson, Mater. Sci. Eng., B **126**, 230 (2006).

[14] O. Gelhausen, E. Malguth, M. R. Phillips, E. M. Goldys, M. Strassburg, A. Hoffmann, T. Graf, M. Gjukic, and M. Stutzmann, Appl. Phys. Lett. **84**, 4514 (2004).

[15] B. Han, R. Y. Korotkov, B. W. Wessels, and M. P. Ulmer, Appl. Phys. Lett. **84**, 5320 (2004).

[16] Z. G. Hu, M. Strassburg, N. Dietz, A. G. U. Perera, A. Asghar, and I. T. Ferguson, Phys. Rev. B **72**, 245326 (2005).

[17] C. Bundesmann, A. Rahm, M. Lorenz, M. Grundmann, and M. Schubert, J. Appl. Phys. **99**, 113504 (2006).

[18] G. Ariyawansa, M. B. M. Rinzan, M. Alevli, M. Strassburg, N. Dietz, A. G. U. Perera, S. G. Matsik, A. Asghar, I. T. Ferguson, H. Luo, A. Bezinger, and H. C. Liu, Appl. Phys. Lett. **89**, 091113 (2006).

[19] A. Kasic, M. Schubert, S. Einfeldt, D. Hommel, and T. E. Tiwald, Phys. Rev. B **62**, 7365 (2000).

[20] M. Holtz, T. Prokofyeva, M. Seon, K. Copeland, J. Vanbuskirk, S. Williams, S. A. Nikishin, V. Tretyakov, and H. Temkin, J. Appl. Phys. **89**, 7977 (2001).

[21] Z. G. Hu, M. Strassburg, A. Weerasekara, N. Dietz, A. G. U. Perera, M. H. Kane, A. Asghar, and I. T. Ferguson, Appl. Phys. Lett. **88**, 061914 (2006).

[22] A. S. Barker, Jr. and M. Ilegems, Phys. Rev. B **7**, 743 (1973).

[23] M. D. Sciacca, A. J. Mayur, E. Oh, A. K. Ramdas, S. Rodriguez, J. K. Furdyna, M. R. Melloch, C. P. Beetz, and W. S. Yoo, Phys. Rev. B **51**, 7744 (1995).

[24] C. Wetzel, E. E. Haller, H. Amano, and I. Akasaki, Appl. Phys. Lett. **68**, 2547 (1996).

[25] M. Schubert, Phys. Rev. B **53**, 4265 (1996).

[26] D. W. Berreman, Phys. Rev. **130**, 2193 (1963).

[27] T. E. Tiwald, J. A. Woollam, S. Zollner, J. Christiansen, R. B. Gregory, T. Wetteroth, S. R. Wilson, and A. R. Powell, Phys. Rev. B **60**, 11464 (1999).

[28] M. Schubert, A. Kasic, T. E. Tiwald, J. Off, B. Kuhn, and F. Scholz, MRS Internet J. Nitride Semicond. Res. **4**, 1 (1999).

[29] G. Yu, N. L. Rowell, and D. J. Lockwood, J. Vac. Sci. Technol. A **22**, 1110 (2004).

[30] H. Harima, J. Phys.: Condens. Matter **14**, R967 (2002).

[31] R. H. Lyddane, R. G. Sachs, and E. Teller, Phys. Rev. **59**, 673 (1941).

[32] F. Gervais and B. Piriou, Phys. Rev. B **10**, 1642 (1974).

[33] W. Gebicki, J. Strzeszewski, G. Kamler, T. Szyszko, and S. Podsiadło, Appl. Phys. Lett. **76**, 3870 (2000).

[34] L. M. Sandratskii, P. Bruno, and S. Mirbt, Phys. Rev. B **71**, 045210 (2005).

[35] A. A. Klochikhin, V. Yu. Davydov, I. N. Goncharuk, A. N. Smirnov, A. E. Nikolaev, M. V. Baidakova, J. Aderhold, J. Graul, J. Stemmer, and O. Semchinova, Phys. Rev. B **62**, 2522 (2000).

[36] M. B. M. Rinzan, A. G. U. Perera, S. G. Matsik, H. C. Liu, Z. R. Wasilewski, and M. Buchanan, Appl. Phys. Lett. **86**, 071112 (2005).

[37] M. Schubert, T. E. Tiwald, and C. M. Herzinger, Phys. Rev. B **61**, 8187 (2000).